ARTICLE

Rotational Spectra of 2,3,6-Trifluoropyridine: Effect of Fluorination on Ring Geometry†

Jun-hua Chen, Juan Wang, Gang Feng, Qian Gou*

Department of Chemistry, School of Chemistry and Chemical Engineering, Chongqing University, Chongqing 401331, China

(Dated: Received on October 22, 2019; Accepted on November 10, 2019)

The ground state rotational spectrum of 2,3,6-trifluoropyridine has been investigated in the 2.0−20.0 GHz region by pulsed jet Fourier transform microwave spectroscopy. The experimental rotational constants are A=3134.4479(2) MHz, B=1346.79372(7) MHz, and C=941.99495(6) MHz. The transitions are so intense that rotational transitions of all mono-^{13}C and ^{15}N isotopologues are measured in natural abundance. The semi-experimental equilibrium rotational constants of the 7 isotopologues were derived by taking account of the anharmonic vibrational corrections, which allowed a semi-experimental determination of the equilibrium structure of 2,3,6-trifluoropyridine.

Key words: 2,3,6-Trifluoropyridine, Fluorination, Semi-experimental structure, Rotational spectra

I. INTRODUCTION

Fluorination of small organic compounds is one of the most common methods to alter their physiochemical characteristics and biological activities, which in some cases are substantially modified in comparison with their non-fluorinated counterparts [1]. For example, the modulation of acidity and lipohilicity, or the control of conformational bias, can be achieved by rational substitution of hydrogen atoms or functional groups by fluorine atoms. Fluorination can also dramatically impact the interaction topologies of other small molecules [3, 4], which can shed light on how fluorination affects the binding affinity and selectivity. Structural information at the molecular level is believed to be essential for understanding the fluorination effects. For this purpose, Fourier transform microwave (FTMW) spectroscopy associated with quantum calculations is especially suitable to describe the molecular geometries by interpreting the corresponding rotational spectra.

Rotational studies of pyridine (PY) [5–10] and its mono-/di-fluorinated derivatives [11–14] yield accurate descriptions of their structural information, which provides an interesting prototype to study the effect of fluorine substitution on the molecular geometry and electronic structure. These studies revealed that fluorination at the *ortho* position gives rise to a more pronounced deviation from the PY ring geometry with respect to the substitution at the *meta* position, which is in agreement with earlier *ab initio* calculations at various levels of theory [15–18]. In addition, the valence angles of the ring at the sites of fluorinations increase by a few degrees for each difluoropyridine (DFPY) with the exception of 23DFPY (less than one degree) with respect to PY. Meanwhile neighboring angles decrease to compensating this change.

Even with small alterations of geometries upon fluorination, the interaction topologies of PY fluorides with water can be quite different [19–22]. It would be interesting to find the border where the interaction topologies change upon multi-fluorination. The alteration on geometries and electronic structures with different fluorination would lay the ground for investigating the microsolvation system. With respect to 23DFPY and 26DFPY [14], we aim to investigate the rotational spectrum of 2,3,6-trifluoropyridine (236TFPY) with pulsed jet Fourier transform microwave technique, which is also the first step towards the investigation of 236TFPY-H_2O.

II. EXPERIMENTS

Rotational spectra of 236TFPY were measured by using the highly integrated pulsed jet FTMW spectrometer [23] (of COBRA-type [24]) built at Chongqing University, covering 2.0−20.0 GHz frequency range and operated with the FTMW++ set of programs [25]. Helium at a backing pressure of about 0.2 MPa passed over the 236TFPY (97%, commercial product from Adamas-Beta used without further purification) and expanded through the solenoid valve (Parker-General Valve, Se-

†Part of the special topic on "the 3rd Asian Workshop on Molecular Spectroscopy"

*Author to whom correspondence should be addressed. E-mail: qian.gou@cqu.edu.cn

DOI:10.1063/1674-0068/cjcp1910184

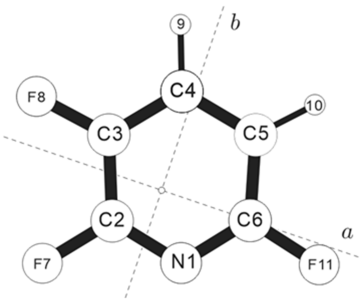

FIG. 1 Molecular structure of 236TFPY with the principal axes and atom numbering.

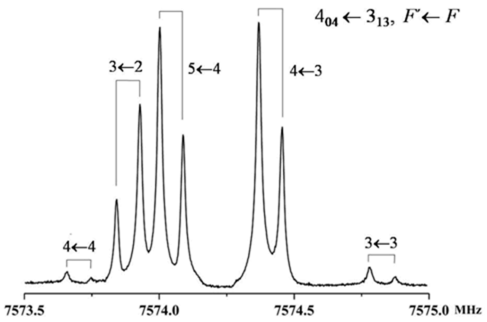

FIG. 2 Recorded 4_{04}-3_{13} transition of 236TFPY showing the ^{14}N nuclear hyperfine structure (64 averages). Each line exhibits the Doppler doubling.

ries 9, nozzle diameter 0.5 mm) into the Fabry-Prot-type resonator. Each rotational transition displays a Doppler splitting that originates from the supersonic jet expanding coaxially along the resonator axis. The rest frequency of the transition line is calculated as the arithmetic mean of the frequencies of the two Doppler components. The bandwidth is 1 MHz, and the spectrum is automatically integrated by each step of 0.4 MHz. The estimated accuracy of the frequency measurements is better than 2 kHz. Lines separated by more than 5 kHz are resolvable.

The rotational spectra of mono-substituted ^{15}N and ^{13}C isotopologues were measured in natural abundance.

III. THEORETICAL CALCULATIONS

To aid the rotational spectrum assignment, geometry optimization of 236TFPY has been performed at the B3LYP/6-311++G(2df,2pd) level of theory by using the Gaussian09 program package [26]. The structure of 236TFPY is shown in FIG. 1, where the principal axes and the atom numbering are also indicated. The resulting spectroscopic parameters are summarized and listed in the first line of Table I. The zero value of the inertial defect (Δ=I_c−I_a−I_b) indicates the planarity of 236TFPY. The dipole moment components are along a- and b-principal inertial axes (μ_a=2.2 D and μ_b=3.3 D).

IV. ROTATIONAL SPECTRA

Following the prediction from the model calculation, a scan has been first performed in the frequency region where the most intense $\mu_{\rm b}$-type transitions would fall. It was easy to identify the R-branch family $(J{+}1)_{0,J+1}{\leftarrow}J_{1,J}$ with J=2 to 10 based on their ^{14}N (I=1) nuclear quadrupole hyperfine structure pattern, as shown in FIG. 2 for the $4_{0,4}{\leftarrow}3_{1,3}$ transition. It was then possible to record more $\mu_{\rm b}$-transitions, including some μ_b-Q branch transitions, from which the rotational constants were well determined. Some less intense $\mu_{\rm a}$-transitions, with rotational quantum number J ranging from 3 to 8 being afterwards measured.

The measured transition frequencies were fitted with Pickett's SPFIT program [27], according to the following Hamiltonian:

$$H = H_{\rm R} + H_{\rm CD} + H_{\rm Q} \quad (1)$$

where $H_{\rm R}$ represents the rigid rotational parts of the Hamiltonian. The centrifugal distortion contributions (analyzed by using the A reduction and $I^{\rm r}$ representation) [28] are represented by $H_{\rm CD}$. $H_{\rm Q}$ is the operator associated with the ^{14}N nuclear quadrupolar interaction. The standard deviation was recalculated with the code PIFORM [29]. Experimental spectroscopic parameters obtained from a non-linear least squares fit are reported in the second line of Table I. The experimental and theoretical rotational constants are in good agreement with the largest discrepancy of ∼0.3%.

After empirical scaling to the rotational constants of the parent species, the rotational spectra of the mono-substituted ^{15}N and ^{13}C isotopologues are possible to be measured and assigned in natural abundance. The transition lines of ^{15}N isotopologue are unsplit due to a ^{15}N nuclear spin quantum number I=1/2. The obtained experimental spectroscopic parameters are reported in Table II. As much fewer transitions were measured, the values of centrifugal distortion constants of the six minor isotopologues were fixed at those of parent species, respectively.

All the measured transition frequencies are available in the supplementary materials.

V. SEMI-EXPERIMENTAL STRUCTURE

Values of inertial defect (Δ) of all isotopologues were calculated from the experimental rotational constants and reported in Tables I and II, respectively, which remain unchanged (all close to zero) upon the isotopic substitutions, as expected for a planar molecule. The small positive values of Δ are typical for planar molecules when there's also the contribution from the vibrational motions in plane [30].

DOI:10.1063/1674-0068/cjcp1910184

TABLE I Experimental and calculated (B3LYP/6-33++G(2df,2pd)) spectroscopic parameters of 236TFPY (A reduction and I^{r} representation).

	A/MHz	B/MHz	C/MHz	χ_{aa}	$\chi_{bb}-\chi_{cc}$	D_J	D_{JK}	D_K	N^{c}	Δ	σ^{d}
Calc.[a]	3142.7	1345.8	942.3	1.346	−6.340	0.0202	0.203	0.32		0.00	
Expt.[b]	3134.4479(2)	1346.79372(7)	941.99495(6)	1.284(1)	−5.853(2)	0.0105(5)	0.116(4)	0.51(2)	45, 185	0.02	3.2

Note: χ in unit of MHz, D in unit of MHz, Δ in unit of uÅ^2, and σ in unit of kHz.
[a] Rotational constants of equilibrium structure.
[b] Uncertainties are standard deviation given (in parentheses) in units of the last digit.
[c] Number of lines in the fit. Two values for each isotopologue are the numbers of unsplit and split lines, respectively.
[d] Standard deviation of the fit.

TABLE II Semi-experimental (SE) rotational constants (in the unit of MHz) of 236TFPY[a].

	A/MHz	B/MHz	C/MHz	χ_{aa}/MHz	$(\chi_{bb}-\chi_{cc})$/MHz	Δ/uÅ^2	N^{c}	σ^{d}/kHz
^{15}N	3114.7306(5)[b]	1345.1935(3)	939.42765(4)			0.02	17, 17	1.2
^{13}C2	3124.4729(1)	1345.5355(2)	940.47728(7)	1.304(8)	−5.848(8)	0.02	15, 41	3.1
^{13}C3	3128.3105(2)	1342.5111(4)	939.3452(1)	1.290(6)	−5.844(4)	0.02	16, 45	2.6
^{13}C4	3084.0598(3)	1346.6748(4)	937.3342(1)	1.271(6)	−5.844(4)	0.02	17, 43	2.7
^{13}C5	3100.3146(7)	1341.9546(4)	936.5347(1)	1.301(5)	−5.868(4)	0.02	17, 49	2.8
^{13}C6	3134.5347(2)	1338.6526(3)	938.0126(1)	1.285(5)	−5.852(4)	0.02	17, 49	2.5

[a] The values of centrifugal distortion constants are fixed at those of the parent species, respectively.
[b] Uncertainties are standard deviation given (in parentheses) in units of the last digit.
[c] Number of transitions in the fit. Two values are the numbers of unsplit and split lines, respectively.
[d] Standard deviation of the fit.

TABLE III Semi-experimental (SE) rotational constants of 236TFPY.

	A_{SE}/MHz	B_{SE}/MHz	C_{SE}/MHz
Parent species	3154.9319	1353.43172	947.13795
N1	3135.1126	1351.7845	944.54065
C2	3144.7399	1352.1185	945.57428
C3	3148.6615	1349.0871	944.4452
C4	3104.2298	1353.2848	942.4452
C5	3120.5266	1348.5546	941.6387
C6	3154.9857	1345.1906	943.0996

The semi-experimental rotational constants of all 7 isotopologues were calculated by taking account the vibrational corrections calculated from the B3LYP/6-311++G(2df,2pd) anharmonic force field, and are reported in Table III. A semi-experimental determination of the equilibrium structure (r_{SE}) was then obtained by a least-squares fit with all the rotational constants being equally weighted [31]. The structural parameters of the heavy-atom frame of 236TFPY are reported in Table IV, with which the semi-experimental rotational constants were then well reproduced, with the largest discrepancy less than 0.003%. The substitution structures (r_{s}) of the six heavy atoms are calculated from Kraitchman's equation [32] and summarized in Table IV, where also the corresponding B3LYP/6-311++G(2df,2pd) calculated coordinates (r_{e}) are given. To have an idea on the structural changes upon trifluorination, the same process was repeated for PY with previous reported rotational results [6], with the same atom numbering of the heavy atoms. The r_{e}, r_{s}, and r_{SE} structures of PY are reported in Table IV. The r_{SE} structure of PY with B3LYP/SNSD vibrational corrections [33] was also summarized in Table IV, where the parameters are in good agreement with this work. B3LYP/6-311++G(2df,2pd) calculated full geometries of PY and 236TFPY are available in the supplementary materials.

The trifluorination causes noticeable shrinking (∼0.03 Å) of the bond length of N1−C2 and N1−C6 bonds. Such results are analogous to those of 2FPY [13], 23DFPY, and 26DFPY [14]. This is most likely due to the electron withdrawing of fluorines which leads to a disruption to the π system. Natural population analyses (NPA) on PY and 236TFPY were performed at the B3LYP/6-311++G(2df,2pd) level of theory to elucidate the electronic transfer upon trifluorination. The charge distributions in PY and 236TFPY are graphically represented in FIG. 3. Trifluorination leads C2, C3, and C6 to be much more positive, while N1, C4, and C5 become slightly more negative. Consequently, the electrostatic attraction N1$\cdots$C2, N1$\cdots$C6, C3$\cdots$C4, and C5$\cdots$C6 increase to a certain degree, *i.e.* the bond lengths are shortened with respect to PY. The C2C3 and C4C5 bonds also show a little bit decrease which might be for the stability of the whole ring structure.

The angles ∠N1C2C3 and ∠C2C3C4 show increases of less than one degree. Such deviations are very similar

DOI:10.1063/1674-0068/cjcp1910184

TABLE IV r_s structures and semi-experimental equilibrium structures (r_{SE}) of PY and 236TFPY.

		R(N1C2)	R(C2C3)	R(C3C4)	R(C4C5)	R(C5C6)	R(C6N1)	R(C2F7)	R(C3F8)	R(C6F11)
PY	r_e[a]	1.343	1.395	1.393	1.393	1.395	1.343			
	r_s[b]	1.336(2)[e]	1.398(3)	1.390(2)	1.390(2)	1.398(3)	1.336(2)			
	r_{SE}[b]	1.336(4)	1.390(3)	1.389(4)	1.389(4)	1.390(3)	1.336(4)			
	r_{SE}[c]	1.3358(5)	1.3907(2)	1.3888(2)	1.3888(2)	1.3907(2)	1.3358(5)			
236TFPY	r_e[a]	1.311	1.391	1.384	1.392	1.387	1.314	1.334	1.342	1.340
	r_s	1.297(3)	1.380(3)	1.385(6)	1.373(8)	1.385(1)	1.322(2)			
	r_{SE}[d]	**1.310(4)**	**1.384(3)**	**1.384(6)**	**1.386(6)**	1.384(6)	**1.312(3)**	**1.321(4)**	**1.336(6)**	**1.327(3)**

		∠(N1C2C3)/(°)	∠(C2C3C4)/(°)	∠(C3C4C5)/(°)	∠(C4C5C6)/(°)	∠(C5C6N1)/(°)	∠(C6N1C2)/(°)
PY	r_e[a]	123.6	118.7	118.3	118.7	123.6	116.9
	r_s[b]	123.7(1)	118.5(1)	118.4(1)	118.5(1)	123.7(1)	117.0(1)
	r_{SE}[b]	123.8(2)	118.5(2)	118.4(2)	118.5(2)	123.8(2)	117.0(2)
	r_{SE}[c]	123.79(3)	118.53(1)	118.44(1)	118.53(1)	123.79(3)	116.93(2)
236TFPY	r_e[a]	123.2	118.5	118.8	116.7	124.9	117.7
	r_s	124.6(2)	117.9(3)	118.7(2)	116.8(1)	125.5(1)	116.5(2)
	r_{SE}[d]	**123.7(2)**	**118.5(2)**	**118.6(1)**	116.8(2)	125.4(2)	**117.0(1)**

Note: R in unit of Å. Error in parentheses in units of the last digit.
[a] B3LYP/6-311++G(2df,2pd) geometries imposed to be planar.
[b] Rotational constants from Ref. [6] used to derived the r_s and r_{SE} structures.
[c] Semi-experimental equilibrium structure with B3LYP/SNSD vibrational [33] for comparison.
[d] The parameters in bold were fit to reproduce the all semi-experimental rotational constants of seven isotopologues of 236TFPY. Errors for r_{SE} are 3σ uncertainties in the least squares fit.

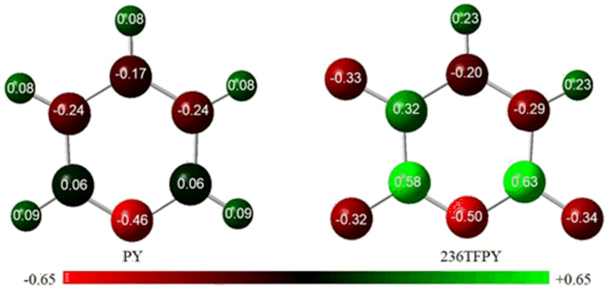

FIG. 3 Charge distributions in PY and 236TFPY.

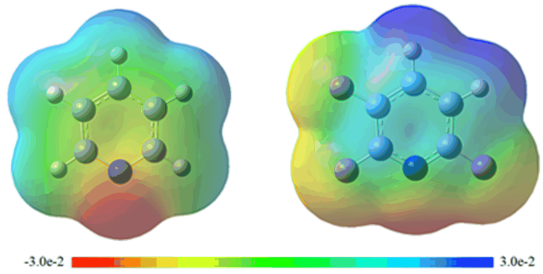

FIG. 4 Electrostatic potential surfaces of PY and 236TFPY. The blue shading is the maximum (positive) potential, and red shading is the minimum (negative) potential.

to those of 23DFPY [14]. It seems that the fluorination on C6 would not lead to any change in the angles of ∠N1C2C3 and ∠C2C3C4 with respect to 23DFPY. The largest difference of valence angles takes place at ∠C5C6N1 with a ∼1.9° increase according to the r_0 structure, which is much smaller than 2FPY [13] or 26DPY [14] with a ∼3° increase. This can be explained by the balance of competing effects for the stability of the ring structure.

VI. ELECTROSTATIC POTENTIAL

To better visualize the electron densities, the molecular electrostatic potential (ESP) analysis was performed for PY and 236TFPY by using Gaussian09 within their B3LYP/6-311++G(2df,2pd) geometries. As indicated in FIG. 4, trifluorination leads to more acidic C−H groups and less electronegativity of N atom. The π-electron density decreases a lot to form a π-hole above the ring, which is slightly positive and could act as the electron acceptor in forming lone-pair$\cdots\pi$ interaction. As a result, when forming complexes with partner molecules, the interaction topologies can be quite different with respect to that of PY.

VII. CONCLUSION

The rotational spectra of seven isotopologues of 236TFPY have been investigated by using the pulsed jet FTMW technique. The structural changes and electron

DOI:10.1063/1674-0068/cjcp1910184

density distributions upon trifluorination are reported for PY and 236TFPY. The *ortho*-fluorination causes the largest shortening of the bond length. Notable increase of the valence bond angle occurs at ∠C5C6N1, which also results in decreases in its adjacent bond angles to compensate for the ring angle opening upon the substitution. Due to electron withdrawing of the fluorine atom, the electron density above the aromatic ring is dramatically reduced upon the trifluorination, which might create new active sites when forming complexes with other molecules.

Supplementary materials: All experimental transition frequencies of 7 isotopologues and the differences between experimental and calculated frequencies of 2,3,6-trifluoropyridine are summarized in Tables S1, S2 and S3). Theoretical geometry of 2,3,6-trifluoropyridine at B3LYP/6-311++G(2df,2pd) level of theory is available in Table S4.

VIII. ACKNOWLEDGMENTS

This work was supported by the National Natural Science Foundation of China (No.21703021 and No.U1931104), the Natural Science Foundation of Chongqing, China (No.cstc2017jcyjAX0068 and No.cstc2018jcyjAX0050), Venture & Innovation Support Program for Chongqing Overseas Returns (No.cx2018064), Foundation of 100 Young Chongqing University (No.0220001104428), and Fundamental Research Funds for the Central Universities (No.106112017CDJQJ228807 and No.2018CDQYHG0009).

[1] C. Heidelberger, N. K. Chaudhuri, P. Danneberg, D. Mooren, L. Griesbach, R. Duschinsky, R. J. Schnitzer, E. Pleven, and J. Scheiner, Nature **179**, 663 (1957).
[2] B. B. Demore, W. S. Wicox, and J. H. Goldstein, J. Chem. Phys. **22**, 876 (1954).
[3] L. Kang, S. E. Novick, Q. Gou, L. Spada, and M. Vallejo-López, J. Mol. Spectrosc. **297**, 32 (2014).
[4] Q. Gou, L. Spada, M. Vallejo-López, L. Kang, S. E. Novick, and W. Caminati, J. Phys. Chem. A **118**, 1047 (2014).
[5] G. O. Sørensen, J. Mol. Spectrosc. **22**, 325 (1967).
[6] G. O. Sørensen, L. Mahler, and N. Rastrup-Andersen, J. Mol. Struct. **20**, 119 (1974).
[7] F. Mata, M. J. Quintana, and G. O. Sørensen, J. Mol. Struct. **42**, 1 (1977).
[8] N. Heineking, H. Dreizler, and R. Schwarz, Z. Naturforsch. **41**, 1210 (1986).
[9] G. Wlodarczak, L. Martinache, J. Demaison, and B. P. Van Eijck, J. Mol. Spectrosc. **127**, 200 (1988).
[10] E. Ye, R. P. A. Bettens, F. C. De Lucia, D. T. Petkie, and S. Albert, J. Mol. Spectrosc. **232**, 61 (2005).
[11] S. D. Sharma, S. Doraiswamy, H. Legell, H. Mäder, and D. Sutter, Z. Naturforsch. **26**, 1342 (1971).
[12] S. D. Sharma and S. Doraiswamy, J. Mol. Spectrosc. **59**, 216 (1976).
[13] C. W. van Dijk, M. Sun, and J. van Wijngaarden, J. Phys. Chem. A **116**, 4082 (2012).
[14] C. W. van Dijk, M. Sun, and J. van Wijngaarden, J. Mol. Spectrosc. **280**, 34 (2012).
[15] M. J. Dewar, Y. Yamaguchi, S. Doraiswamy, S. D. Sharma, and S. H. Suck, Chem. Phys. **41**, 21 (1979).
[16] J. E. Del Bene, J. Am. Chem. Soc. **101**, 6184 (1979).
[17] J. E. Boggs and F. Pang, J. Heterocycl. Chem. **21**, 1801 (1984).
[18] P. Boopalachandran, S. Kim, J. Choo, and J. Laane, Chem. Phys. Lett. **514**, 214 (2011).
[19] R. B. Mackenzie, C. T. Dewberry, R. D. Cornelius, C. J. Smith, and K. R. Leopold, J. Phys. Chem. A **121**, 855 (2017).
[20] Q. Gou, L. Spada, M. Vallejo-Lopez, S. Melandri, A. Lesarri, E. J. Cocinero, and W. Caminati, ChemistrySelect **6**, 1273 (2016).
[21] C. Calabrese, Q. Gou, L. Spada, A. Maris, W. Caminati, and S. Melandri, J. Phys. Chem. A **120**, 5163 (2016).
[22] C. Calabrese, Q. Gou, A. Maris, W. Caminati, and S. Melandri, J. Phys. Chem. Lett. **7**, 1513 (2016).
[23] T. J. Balle and W. H. Flygare, Rev. Sci. Instrum. **52**, 33 (1981).
[24] J. U. Grabow, W. Stahl, and H. Dreizler, Rev. Sci. Instrum. **67**, 4072 (1996).
[25] J. Chen, Y. Zheng, J. Wang, G. Feng, Z. Xia, and Q. Gou, J. Chem. Phys. **147**, 094301 (2017).
[26] M. J. Frisch, G. W. Trucks, H. B. Schlegel, G. E. Scuseria, M. A. Robb, J. R. Cheeseman, G. Scalmani, V. Barone, B. Mennucci, G. A. Petersson, H. Nakatsuji, M. Caricato, X. Li, H. P. Hratchian, A. F. Izmaylov, J. Bloino, G. Zheng, J. L. Sonnenberg, M. Hada, M. Ehara, K. Toyota, R. Fukuda, J. Hasegawa, M. Ishida, T. Nakajima, Y. Honda, O. Kitao, H. Nakai, T. Vreven, J. A. Montgomery, Jr., J. E. Peralta, F. Ogliaro, M. Bearpark, J. J. Heyd, E. Brothers, K. N. Kudin, V. N. Staroverov, R. Kobayashi, J. Normand, K. Raghavachari, A. Rendell, J. C. Burant, S. S. Iyengar, J. Tomasi, M. Cossi, N. Rega, J. M. Millam, M. Klene, J. E. Knox, J. B. Cross, V. Bakken, C. Adamo, J. Jaramillo, R. Gomperts, R. E. Stratmann, O. Yazyev, A. J. Austin, R. Cammi, C. Pomelli, J. W. Ochterski, R. L. Martin, K. Morokuma, V. G. Zakrzewski, G. A. Voth, P. Salvador, J. J. Dannenberg, S. Dapprich, A. D. Daniels, Ö. Farkas, J. B. Foresman, J. V. Ortiz, J. Cioslowski, and D. J. Fox, *Gaussian 09, Revision A.02*, Wallingford CT: Gaussian Inc., (2009).
[27] H. M. Pickett, J. Mol. Spectrosc. **148**, 371 (1991).
[28] J. K. G. Watson, *Vibrational Spectra and Structure*, J. R. Durig Ed., New York: Elsevier, 1 (1977).
[29] Z. Kisiel, PROSPE-Programs for Rotational SPEctroscopy, http://www.ifpan.edu.pl/∼kisiel/asym/pickett/crib.htm#errors.
[30] T. Oka, J Mol. Struct. **352/353**, 225 (1995).
[31] Z. Kisiel, PROSPE-Programs for Rotational SPEctroscopy, http://info.ifpan.edu.pl/∼kisiel/prospe.htm.
[32] J. Kraitchman, Am. J. Phys. **21**, 17 (1953).
[33] M. Piccardo, E. Penocchio, C. Puzzarini, M. Biczysko, and V. Barone, J. Phys. Chem. A **119**, 2058 (2015).

DOI:10.1063/1674-0068/cjcp1910184